SIMULATION OF USING ORBIT BUMPS TO TEST SEXTUPOLE COMPENSATION FOR THE SHORT PULSE X-RAY SYSTEM AT THE ADVANCED PHOTON SOURCE *

M. Borland[†], V. Sajaev, ANL, Argonne, IL 60439, USA

Abstract

As part of an ongoing upgrade of the Advanced Photon Source (APS), a Short Pulse X-ray (SPX) system is being developed based on two sets of crab cavities separated by 180 degrees vertical phase advance. Emittance growth due to incomplete cancellation of the kicks from the sets of cavities is a concern. Simulations predict that it can be controlled by adjustment of the sextupoles between the cavities. To test these predictions, we can use orbit bumps that reproduce the trajectories of individual particles through the sectors in question. We present results of simulations of such tests, showing the degree to which the emittance growth and other properties of the machine will differ for optimized and unoptimized sextupoles. We also show results of recent experimental tests.

INTRODUCTION

One of the challenges of operating the Short Pulse X-ray (SPX) facility [1, 2] will be preserving the small vertical size of the APS beam. Vertical emittance increase was predicted in early simulations of SPX [3]. It results mainly from additional coupling occurring due to large vertical trajectories in sextupoles between the SPX cavities [4]. This emittance increase is undesirable because it decreases the x-ray brightness seen by all users. It also increases the minimum x-ray pulse duration that SPX can deliver.

We also found that lifetime and injection efficiency were negatively affected by this strong local coupling through stronger excitation of nearby nonlinear resonances. We resolved these problems in simulation by optimizing the sextupoles between the SPX cavities so as to minimize the vertical emittance growth, while at the same time preserving injection efficiency and lifetime [5].

Owing to the expense and complexity of SPX, it is desirable to test as many aspects of the beam dynamics ahead of time. With deflecting cavities, every longitudinal slice of the beam travels on its own vertical trajectory. The amplitudes of those trajectories depend on the longitudinal position of the slice. Without deflecting cavities, we cannot recreate this behavior completely, but we can generate a real orbit bump using orbit correctors where the entire beam would go on a trajectory corresponding to some beam slice. We could thus verify that the effect of the orbit bump on coupling and nonlinear dynamics is reduced when properly optimized sextupoles are used.

Any two vertical correctors bracketing a straight section can be used to produce a trajectory that exactly corresponds to a trajectory originating from a single vertical kick somewhere in the straight section. Using existing correctors powered at modest levels, we can simulate deflections equivalent to a cavity deflecting voltage of about 4 MV without loss of stored beam. Note that this is a very stringent test, not only because it exceeds the intended maximum deflection by a factor of two, but because with actual deflecting cavities, very few electrons experience deflections that are close to the maximum possible deflection, owing to the small $33°$ rms phase spread of the bunch.

LATTICE OPTIMIZATION

The lattices used for the simulations and experiments are mock-ups of the planned operational lattices. The latter will differ from today's lattice by long straight sections (LSS) in straight sections 1, 5, and 7, as well as a special insertion with reduced horizontal beam size (RHB) in straight section 20. Two of the LSSs (in straights 5 and 7) are associated with SPX, being required in order to make room for the cryomodules. The vertical phase advance between these straights (i.e., through sectors 6 and 7) is ideally 2π. The LSSs are mocked up by setting to zero certain magnets that would be removed to make an actual long straight.

The tests require two lattices: one in which the sextupoles in sectors 6 and 7 are optimized to minimize SPX emittance growth, and a second with normal sextupoles in those sectors. The first lattice was optimized using a direct genetic algorithm [6] with fictitious zero-length crab cavities located located 1.2 m downstream of the center of straight sections 5 and 7. The cavities were powered at 2-MV deflection strength during the optimization of dynamic aperture, lifetime, and vertical emittance growth. The optimization was very effective, giving a nominal lifetime of over 11 hours for 24 bunches, 100 mA, 1% coupling, and $\xi_x = \xi_y = 5$; dynamic acceptance of -15 mm; and emittance growth of less than 1 pm on a base of 35 pm.

The second lattice started from the first, but the sextupoles in sectors 5 and 7 were identical to those in sector 1, while the sextupoles in sectors 6 and 8 were identical to those in sector 2. This condition results from the fact that straight sections 1, 5, and 7 are all long straights. This optimization also worked well, but not as well as the previous one, which is perhaps not surprising given that it had fewer knobs with which to work. The lifetime was just under 10 hours, with dynamic acceptance beyond -15 mm.

SIMULATION RESULTS

The purpose of the simulations is to determine whether we can realistically expect to measure differences between the two lattices. Lacking a calibrated model for these lattices, we used 500 random error ensembles, with realistic error levels, with the quadrupole tilt error level chosen to give a vertical emittance of about 10 pm. The vertical emittance was computed for each ensemble using the 6D equilibrium beam moments computation in `elegant` [7]. However, some ensembles gave much higher vertical emittance, so we selected those ensembles giving a vertical emittance of 10 to 15 pm for use in the remaining simulations. For the uncompensated lattice, we had 140 ensembles left, while for the compensated lattice we had 127.

For each ensemble, we performed simulations with bump amplitudes up to 4 MV equivalent. Figure 1 shows the Courant-Snyder invariant of the orbit outside the bump vs voltage for the two cases. Even for 4 MV equivalent, the error bars nearly overlap, indicating that bump leakage is not a reliable way to distinguish between the lattices.

The conclusion is more promising for the vertical emittance, as shown in Figure 2. Here we see that at the 2-MV level the two cases will be separated by a significant gap. Hence, we can expect to see a significant difference when we perform experiments.
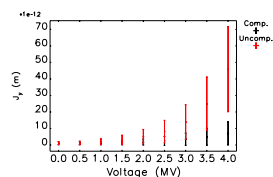

Figure 1: Courant-Snyder invariant vs equivalent deflecting voltage for lattices with and without compensated sextupoles, for many error ensembles.
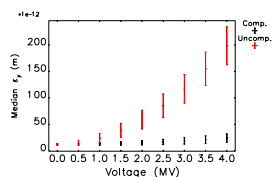
Figure 2: Median vertical emittance vs. equivalent deflecting voltage for lattices with and without compensated sextupoles, for many error ensembles.

We also simulated the dynamic acceptance (DA) and local momentum acceptance (LMA) [8], and computed the Touschek lifetime from the latter. These are to be seen from a different perspective, since we do not expect the configuration with compensated sextupoles to perform as well as the uncompensated case. The compensation is required to reduce the vertical emittance and is designed to have an acceptably small impact on nonlinear dynamics. In comparison to the last set of calculations, these are far more CPU intensive. Hence, we performed runs for only five values of voltage from 0 to 4 MV. In addition, for the LMA computations we used only 50 of the ensembles (subject to the same selection process described above).

For dynamic acceptance, we used all the available ensembles (subject to the vertical emittance limit described above). We tracked 400 turns using parallel `elegant` [9] with kick elements, rf, and lumped synchrotron radiation.

Figures 3 and 4 show the DA for the compensated and uncompensated cases. We see that up to 3 MV, the DA is maintained at nearly the level for the uncompensated case, dropping signicantly for both cases at 4 MV.
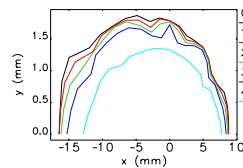

Figure 3: Median dynamic acceptance for case with compensated sextupoles as a function of equivalent deflecting voltage.
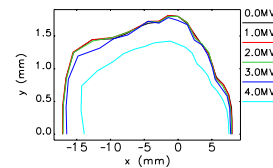
Figure 4: Median dynamic acceptance for case with uncompensated sextupoles as a function of equivalent deflecting voltage.

Simulations of the LMA show that the uncompensated case is significantly worse as the equivalent voltage is increased, which is not surprising [5]. However, when we compute the Touschek lifetime for each ensemble using `touschekLifetime` [10], including the inflated emittances computed above, we see that the lifetime is significantly longer for the uncompensated case, as seen in Figure 5. This is a result of the larger vertical emittance, and hence this measurement would add nothing new.

The momentum acceptance can be measured more directly by scanning the main rf voltage V_m. Figure 6 show the momentum acceptance as a function of equivalent deflecting voltage. The difference of more than 0.2% in momentum acceptance for an equivalent voltage of 3 MV corresponds to the difference between 8.2 and and 8.7 MV in V_m, which should be measurable.
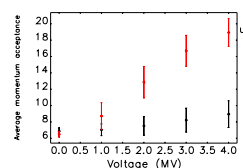

Figure 5: Touschek lifetime as a function of equivalent deflecting voltage for compensated and uncompensated sextupoles.
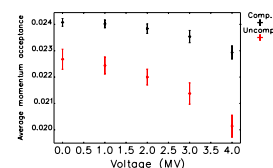
Figure 6: Average momentum acceptance as a function of equivalent deflecting voltage for compensated and uncompensated sextupoles.

EXPERIMENTAL RESULTS

The mock-up lattices desribed above were set up during storage ring studies, using the so-called "reference" orbit, which goes through the centers of magnets rather than accommodating user steering. Figure 7 shows the beta functions after the lattice setup was completed for the lattice with compensated sextupoles.
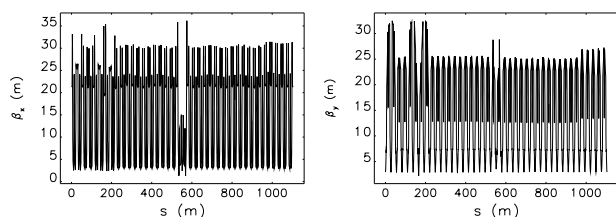
Figure 7: Beta functions of the lattice with compensated sextupoles as measured by the response matrix fit after optics correction.

We used pairs of A:V1 and B:V1 correctors bracketing straight sections 5 and 7 to generate the orbit bumps. The ideal corrector settings nearly closed orbit bumps, with maximum orbit distortion outside the bump of only 2% of the bump amplitude. To improve the bump closure further, we decided to change manually only the pair of correctors around straight section 5 while the other pair of correctors was controlled by orbit feedback.

According to the simulations presented above, the biggest distinction between the lattices shows up in the vertical emittance—and therefore beam size—dependence on the orbit bump amplitude. We performed scans of the bump amplitude for both sets of sextupoles and recorded the beam sizes. Figure 8 shows the dependence of the vertical beam size on the orbit bump amplitude, which is presented in the units of the equivalent deflecting voltage. This plot should be compared with Figure 2. As expected, the lattice with compensated sextupoles shows almost no beam size dependence on the deflecting voltage amplitude, while the lattice with uncompensated sextupoles shows strong dependence. This measurement has verified that the emittance growth can be controlled by optimizing sextupoles.
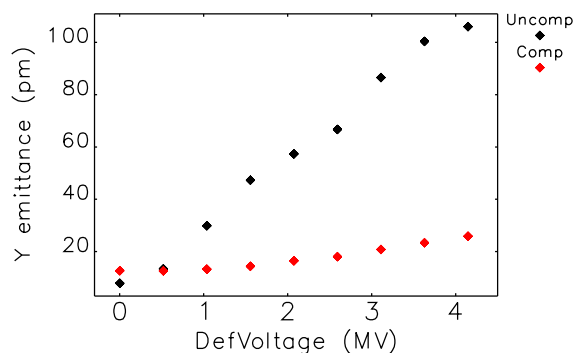

Figure 8: Measured vertical emittance dependence on the equivalent deflecting voltage for lattices with and without compensated sextupoles.

We also measured lifetime and injection efficiency as a function of the orbit bump amplitude. Figures 9 and 10 show the results. Simulations predict that for the lattice with compensated sextupoles the lifetime should not change significantly in the range of deflecting voltage up to 4 MV (see Figure 5). In our measurements, the lifetime

stayed approximately constant for the orbit bumps corresponding to deflecting voltage in the range from -4 MV to +3 MV, which roughly corresponds to the predictions.

We have not directly measured the dynamic acceptance of the lattices. However, we have recorded injection efficiency, which can be used as a measure of the dynamic acceptance since our efficiency is defined mostly by the dynamic acceptance of the storage ring. The dynamic acceptance simulations show no big effect for voltages up to 3 MV and then a reduction for 4 MV (Figures 3 and 4). The measurements gave us good injection in the range of orbit bumps corresponding to voltages from -4 MV to +2.5 MV. This again roughly corresponds to simulations.
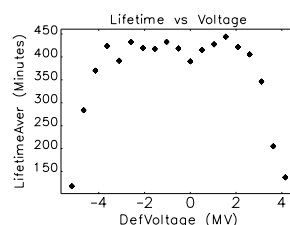

Figure 9: Lifetime as a function of the orbit bump amplitude presented in units of the deflecting voltage for compensated sextupoles.
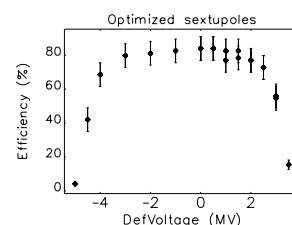
Figure 10: Injection efficiency as a function of the orbit bump amplitude for the compensated sextupoles.

CONCLUSIONS

We performed simulations and experiments to investigate whether use of closed orbit bumps is a valid way to simulate the sextupole compensation scheme for SPX. In simulation, we found that vertical emittance and, to a lesser extent, momenmtum aperture, should show a measurable difference between the two configurations. Experiments verified that the emittance growth is controlled by the compensating sextupoles.

REFERENCES

[1] A. Zholents, R. Heimann et al., NIM A 425, 385 (1999).

[2] A. Nassiri et al., IPAC 2012, 2292 (2012).

[3] M. Borland, PRSTAB 8(7), 074001 (2005).

[4] M. Borland and V. Sajaev, PAC 2005, 3886 (2005).

[5] APS Upgrade Preliminary Design Report (2012), Chapter 3.2.2.4.

[6] M. Borland, V. Sajaev et al., ANL/APS/LS-319, APS (2010).

[7] M. Borland, ANL/APS/LS-287 (2000).

[8] M. Belgrounne et al., PAC 2003, 896 (2003).

[9] Y. Wang, M. Borland et al., ICAP 2009, 355 (2009).

[10] A. Xiao and M. Borland, PAC 2007, 3453–3455 (2007).